LA-UR-94-3350

Conf-9410219--22

TITLE: # NONINTERCEPTIVE BEAM ENERGY MEASUREMENTS IN LINE D OF THE LOS ALAMOS MESON PHYSICS FACILITY

AUTHOR(S): John D. Gilpatrick
Hamilton Carter
Mike Plum
John F. Power
Chris R. Rose
R. Brad Shurter

SUBMITTED TO: Beam Instrumentation Workshop
Vancouver, B. C., Canada
October 2-6, 1994

DISCLAIMER

Noninterceptive Beam Energy Measurements in Line D of the Los Alamos Meson Physics Facility*

J. D. Gilpatrick, H. Carter, M. Plum, J. F. Power, C. R. Rose, R. B. Shurter
Los Alamos National Laboratory, M. S. H808, Los Alamos, NM, 87545

Abstract

Several members of the Accelerator and Operations Technology (AOT) division beam-diagnostics team performed time-of-flight (TOF) beam-energy measurements in line D of the Los Alamos Meson Physics Facility (LAMPF) using developmental beam time. These measurements provided information for a final design of an on-line beam energy measurement. The following paper discusses these measurements and how they apply to the final beam energy measurement design.

INTRODUCTION

The purpose of the beam measurements performed was to provide information for the design and implementation of an on-line beam-energy measurement system with sufficient bandwidth, resolution, and repeatability to monitor the beam energy as beam is injected into the proton storage ring (PSR). Using existing probes, cables, and ground test accelerator (GTA) processing electronics, we were able to monitor the relative beam energy using TOF techniques. This simple technique measures the time that a particular beam bunch travels between two image-current beam probes separated by a known distance. The time measurement is accomplished by measuring the phase difference of the 201.25-MHz probe signals. This technique has the advantage that it does not intercept or perturb the beam and has a wide overall bandwidth.

As the beam measurements were performed, three questions were answered.

1.) With the approximate 25-m drift distance in a straight portion of the LAMPF Line D, is there sufficient energy-measurement resolution for monitoring the PSR injected beam using a TOF measurement system?

2.) What influence does the beam chopping have on the design of the TOF processing electronics?

3.) Does changing the beam position or trajectory angle upstream of this portion of Line D change the flight path of the beam enough to limit the TOF measurement system repeatability?

EXPERIMENT DESCRIPTION

The measurement system used was a combination of microstrip- or stripline-style beam position monitors (BPM) already installed in Line D, 3/8" heliax already installed into the facility, and two altered microstrip-measurement-system electronics used in the GTA (1). The probes were a standard 10-cm aperture, 36°-

---

* Work supported in part by the US Department of Energy, Office of Defense Programs and in part by the Los Alamos Laboratory Institutional Supporting Research.

subtended angle, 34-cm long lobe probes that have been used for some time at LAMPF/PSR. The distance between probes is 24.77 ± 0.01 m.

Using the existing heliax cables, two sets of GTA-based microstrip processing-electronics were connected to these cables. Each of the probes then had horizontal and vertical beam positions, beam intensities, and a single TOF channel. A block diagram of a typical GTA microstrip processing electronics is shown in Fig. 1.

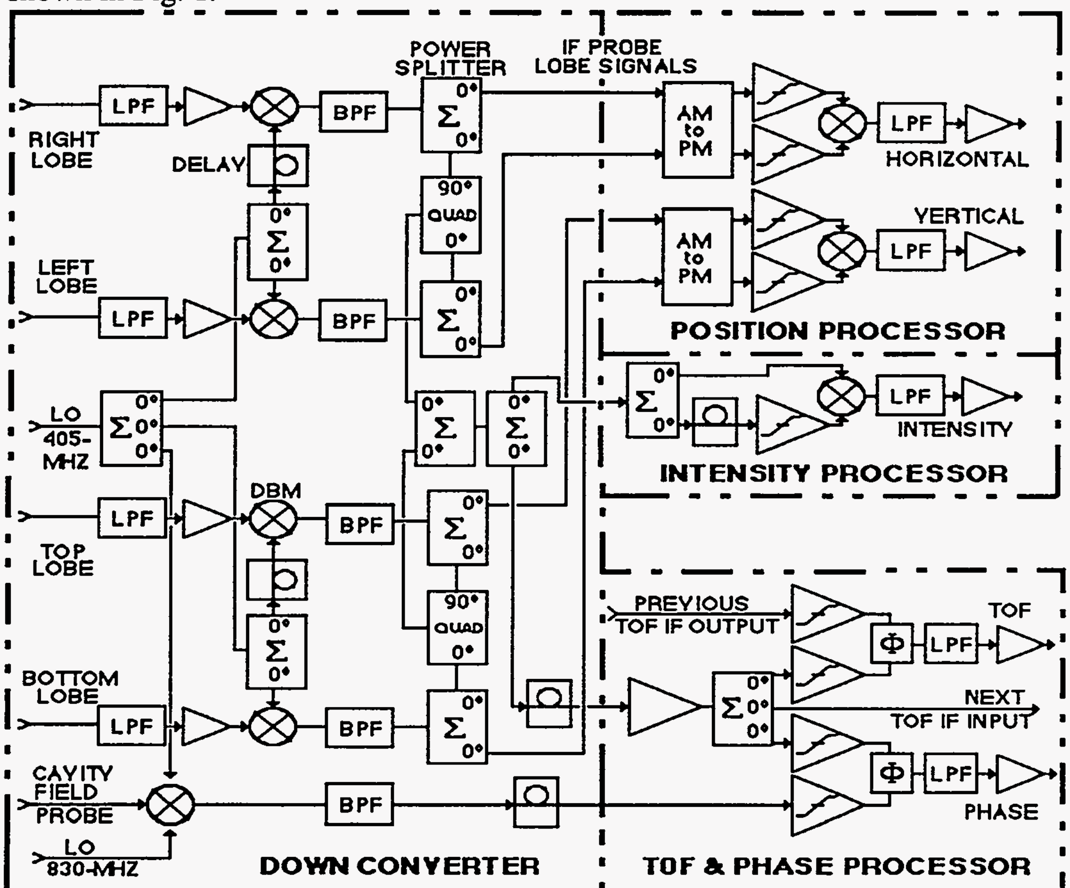

Figure 1. Typical block diagram of the GTA microstrip system showing the beam output phase, energy/TOF, position, and intensity measurements. The component identified as BPF, LPF, LO, and DBM are bandpass filters, lowpass filters, local oscillator, and double balanced mixers, respectively.

The GTA bunching and local oscillator frequencies were 425- and 405-MHz, respectively. These radio frequencies produced an intermediate frequency (IF) of 20 MHz. The overall system bandwidth was 2 MHz. For our tests, we changed the input lowpass filter corner frequency to 240 MHz and the local oscillator to 181.25 MHz so that the rest of the system (i.e., IF bandpass filters, etc.) did not need to be changed. For these measurements, the output-phase portion of this circuitry was not used. The data were acquired locally with the combination of a LeCroy 9400 oscilloscope connected to a Macintosh computer running National Instrument's Labview data acquisition and analysis software. Since the peak beam current was typically 7.7 mA, the peak signal power during the macropulse was 10 dB from the top of the 34-dB dynamic range of the TOF processing electronics. Table 1 lists the beam parameters used during the experiment.

Table 1. Beam parameters used during the three experimental measurement sets.

Parameter	Set #1	Set #2	Set #3
Average Current during Macropulse (mA)	7.7	5.3 to 1.3	7.7
Chopping Pulse Length (μs)	none	0.25	none
Chopping Pulse Repetition Rate (kHz)	none	2795	none
Countdown Number	none	1 to 4	none
Macropulse Length (ms)	0.65	0.65	0.15
Macropulse Repetition Rate (Hz)	1	1	1

EXPERIMENTAL DATA

The experiment consisted of three sets of measurements:

1) TOF measurements versus linac module-48 cavity-phase as the cavity phase is varied;

2) TOF processor output signal acquired and analyzed as the countdown is varied; and

3) TOF measurements versus beam position and trajectory-angle as the beam position and trajectory angle are varied.

During the first set of measurements, the relative beam energy was monitored with the TOF energy measurement and a wire scanner beam profile measurement. The wire scanner horizontal-profile measurement is in the middle of an 89° bend in the beam transport where the dispersion is high (i.e., 50±0.5 mm per % of $\Delta p/p$). Therefore, as the beam energy changes, the centroid of the beam's horizontal distribution changes. The wire scanner measurement is upstream of the first probe of the TOF energy measurement and both measurements are downstream from the last linac accelerating structure, module 48.

In order to get a general sense of the operational characteristics of the TOF measurement, the central beam energy was changed and the measured beam energy and single particle simulation was compared. This technique is commonly known as a "phase scan". Following a typical phase scan procedure, the cavity phase of module 48 was changed by ±10° about the synchronous phase in 2° steps. At each step, wire scanner and TOF energy measurement data were acquired. These data were then normalized to 799.795 MeV and plotted in Fig. 2 and 3. The important information is in the slope and shape of the fitted polynomial curves. The TOF and wire scanner measurements appear to track each other fairly well. The relationship between the two measurements may be further compared if the TOF data are plotted as a function of the wire scanner data (see Fig. 3). Note that the two energy measurements agree within approximately 3%.

Noise data were also taken using an external 201.25-MHz oscillator as a beam-induced input-signal replacement to the down-converter and TOF processing electronics. A power meter whose bandwidth lies between 3-Hz and 300-kHz was used to measure the TOF output-signal noise. These bench data indicated that the precision of the measurement processing electronics is approximately ±0.2 mV or ±0.1 ps over a 15-dB portion of the dynamic range. This is equivalent to ±4 keV of beam energy over a 4- to 22-mA beam current range. However, the expected signal-to-noise ratio must also be estimated and added appropriately to the measurement resolution. If reasonably conservative estimates of the noise floor

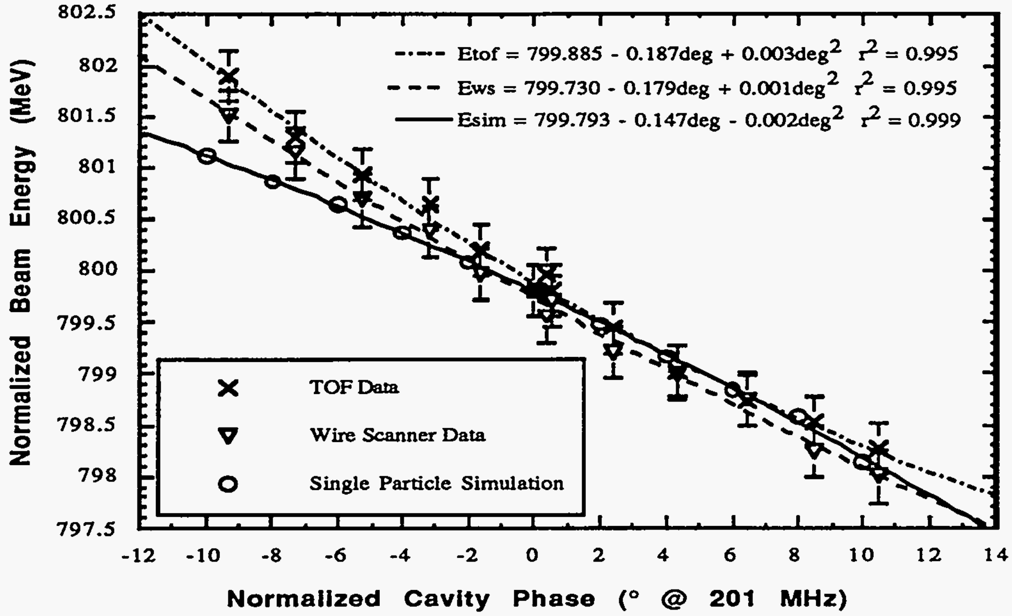

Figure 2. TOF and wire scanner energy measurement data plotted as a function of normalized cavity phase. Both energy measurements were normalized to a single-particle-simulation synchronous energy (also plotted). Error bars indicate the amount of beam energy jitter. TOF energy-measurement resolution is approximately ±7-keV and wire scanner energy-measurement resolution is approximately ±62-keV. The lines are a least-squares second-order fit to the data where each fitted equation and its associated correlation coefficient, r^2, is given.

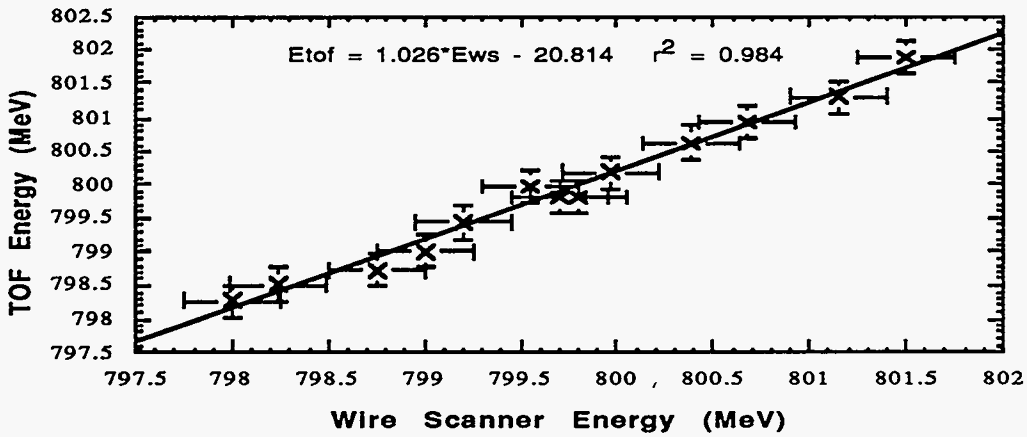

Figure 3. This graph plots the correlation between the two energy measurements.

(-91-dBm) are assumed, the measured -15-dBm probe-signal power produces an overall resolution estimate of ±7 keV. This is better than what will likely be required for the final energy measurement.

For the second set of measurements, the TOF, intensity, and beam-position output signals from both probes were digitized. The important TOF information is contained in a very small bandwidth about 201.25 MHz probe-signal components. As can be seen in Fig. 1, this information is down-converted to 20 MHz and then detected to an overall bandwidth of DC to 2 MHz. The output signals were sampled with 1000 points across a 5-μs section of the macropulse approximately 250 μs into the macropulse. Chopping countdowns from 1 through 4 were applied to the beam. This chopping pattern is generated to provide proper timing for the PSR injected beam. The chopping frequency is the 72^{nd} sub-harmonic of the 201.25-MHz beam-bunching frequency (or approximately 2.8 MHz). The chopped beam structure for a countdown of 1 is 250 ns of beam and a 110-ns gap. As the chopping countdown is increased, 250-ns chopped beam pulses are removed. For example, a countdown of 3 produces 250-ns chopped beam pulses every 1080 ns (i.e., 830 ns gap between chopped beam pulses). The data were then windowed with a Hamming data window and padded with zeros so that the vector length was 1024 points. These time domain data were then transformed to the frequency domain using a fast Fourier transform (FFT). The complex vector was then transformed to magnitude information and the resulting low-frequency portion of the transformed information is displayed in Fig. 4.

One technical design aspect for the final energy measurement is how to deal with the beam chopping characteristic of the PSR-injected beam. The beam chopping produces gaps within the macropulse, during which there is no beam. In the TOF electronics, when there is no beam, the limiters do not have any signal to "lock-on" and will randomly oscillate between their plus and minus power supply voltages. These oscillations would drastically compromise the resolution and repeatability of the measurement. However, it is possible to choose the IF bandpass filter characteristics (i.e., bandwidth, center frequency, etc.) so that the 2.8-MHz chopping frequency does not effect the TOF output signal.

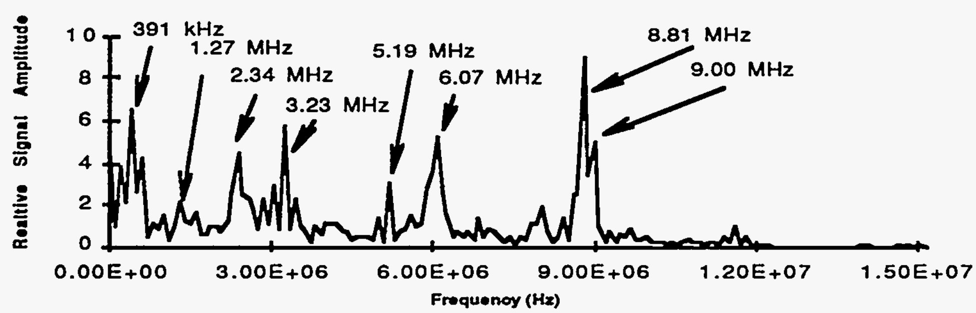

Figure 4. FFT of TOF output signal for countdown-of-1 data.

This figure shows that not only do we need to be concerned with the fundamental 2.8-MHz component, we also need to consider the harmonics of this chopping frequency. For example, a modulation product from the 7^{th} harmonic (i.e., 7x2.8-MHz=19.56-MHz) of the 2.8-MHz chopping frequency and the 20-MHz IF frequency component produces a 434-kHz frequency component at the TOF output-signal port. Since the frequency domain resolution for Fig. 4 is approximately 98 kHz, the 434-kHz component is reflected by noting the presence of a 391-kHz component. Because the bandpass and lowpass filters in the processing electronics have limited bandwidths of below 3 MHz, the higher frequency components between 3- and 12-MHz appearing in Fig. 4 were not initially expected. However, it was discovered that these components are due to the presence of two primary modulation products from the down-converted probe signals, 19.56- and 22.36-MHz. The TOF phase detector demodulates these two products and produces many "daughter" products of sizable magnitude relative to the fundamental beam information. Therefore, there are two separate demodulation processes occurring that produce the spectrally rich signals shown in Fig. 4. The first process produces the fundamental modulation products below 3 MHz and the second process produced by the phase detector in the TOF electronics processor manufactures "daughter" or second generation products. Because the lowpass filters TOF processing electronics were not designed for these chopped beam signals, these spectrally rich signals are seen at the TOF output-signal ports. It is clear that for the final measurement it will be important to pick the IF bandpass filter center frequency, bandwidth, etc. so that all of the modulation products are outside the filter's bandwidth for all operational countdown conditions.

For the final measurement set, the beam was steered in the horizontal and vertical axes with steering magnets upstream of the two line-D probes. A change in these steering magnet settings will result in a change in the beam trajectory in the magnetic transport elements between the two beam probes. There are no steering or dipole magnets between the two probes but there are three sets of quadrupole doublets. The procedure used to change the beam position and angle was that the operators changed a magnet setting until the beam loss measurement between the two microstrip probes reached a maximum acceptable level. This was done for both directions from the nominal trajectory and for both axes. The steering data are shown in Fig. 5. The vertical data shows little vertical position change. The horizontal magnet steered the beam slightly under 15 mm at the first probe and approximately 6 mm at the second probe.

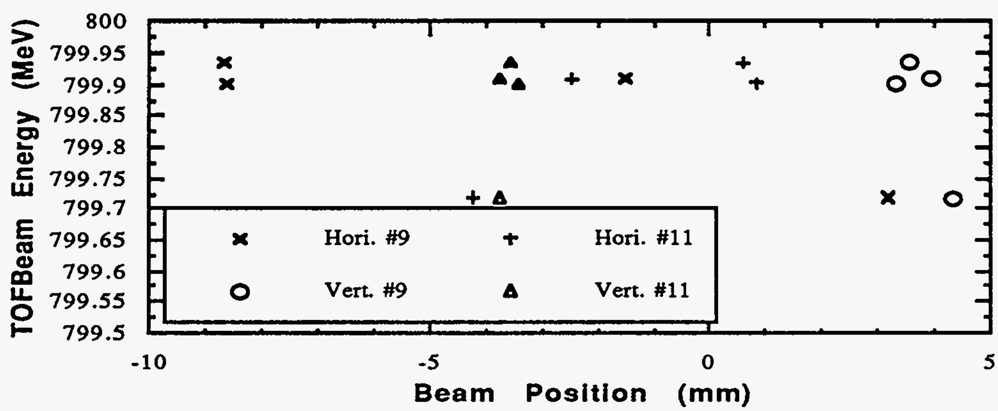

Figure 5. This graph shows the measured beam energy versus the horizontal and vertical steered beam for both probes. Data are averaged over 20 macropulses.

The amount of energy change for the horizontal data shown in Fig. 5 is approximately 200-keV. How does this compare with first order theory? Assume a worst case condition in which at each of the doublets between the two probes, the beam trajectory is offset 30 mm from beamline center (beampipe diameter is 100 mm) in a zig-zag fashion. This offset beam trajectory changes the path length from a centered-beam trajectory by approximately 0.65 mm. Substituting this error into Eq. 1 and solving for the energy error,

$$\Delta E = -\frac{(\beta\gamma)^3 mc^2 \lambda_0}{L}\left[\frac{\Delta\varphi}{2\pi} - \frac{\Delta L}{\beta\lambda_0}\right] \quad (1)$$

where β is the relative beam velocity, γ is the Lorentz contraction factor, L is the drift distance, mc^2 is the rest energy of the accelerated particle, ΔL and $\Delta\varphi$ are the distance and phase errors, and λ_0 is the free space wavelength of the bunching frequency.(2) The resultant error is 110 keV. The measured steering data shown in Fig. 5 are within a factor of 2 of this calculated energy error.

Several indications throughout the experiment corroborate the observation that beam energy jitter larger than the steered-beam energy change was present during the experiment. Both of the energy measurements shown in Fig. 2 have approximately the same amount of error or jitter - approximately ±250 keV. During this initial measurement set, the module 48 cavity power and field amplitude were recorded several times for the nominal set points. The field amplitude varied by 0.3% and the cavity and waveguide power (i.e., forward minus the reflected power) varied by 10-kw out of 830-kw. These variations in module 48 cavity power alone could account for variations in beam energy of 60- to 120-keV. In total, all of these observations seems to indicate that an energy jitter of approximately 300- to 500-keV was present throughout the experiment.

CONCLUSION

Using the existing probes, cables, and GTA TOF processing-electronics, resolutions of 7 keV were estimated based on the 25-m drift distance, bench noise measurements and expected beamline noise. This estimated resolution is much better than will likely be required for the final beam energy measurement. Phase scans were acquired using TOF- and wire-scanner-based energy measurements with good agreement between the two types of measurements. Under chopped beam conditions, good agreement was found between TOF output signal data and theory. These chopping effects will guide the design of the processing electronics and the choice of the bandpass and lowpass filter specifications. TOF flight-path lengths do change as a function of beam steering in this particular beamline. However, the data and simple theory indicate that the change of energy due to the path length change is less than will be required for the final measurement. Based on these initial measurements, an 800-MeV TOF beam-energy measurement in this facility is feasible.

REFERENCES

1. J. D. Gilpatrick, et. al., "Experience with the Ground Test Accelerator Beam-Measurement Instrumentation," presented at the Beam Instrumentation Workshop, Santa Fe, NM, October, 6-12, 1993.
2. J. D. Gilpatrick, et. al., "Beam Energy Measurements in Line D," Los Alamos National Laboratory Technical Note, AOT-3:TN:94-18, September, 1994.